

Anther and pollen development in the lodgepole pine dwarf mistletoe (*Arceuthobium americanum*) staminate flower

Kaitlyn C. Munro, Jeffrey R.M. Jackson, Ivan Hartling, Michael J. Sumner, and Cynthia M. Ross Friedman

Abstract: The lodgepole pine dwarf mistletoe, *Arceuthobium americanum* Nutt. ex Engelm., is a parasitic angiosperm that infects conifers in western Canadian forests. While production of viable pollen in anthers is critical to dwarf mistletoe reproduction, the few existing reports that examine staminate development in *Arceuthobium* are often incomplete or conflicting. The objective of this work was to investigate the developmental anatomy of anther and pollen of *A. americanum* using modern microscopy. We found that the microsporangium was toroidal from the outset and gave rise to a central peg-shaped sterile “columella” early in anther development. The endothecium was absent, the epidermis persisted as an “exothecium” fulfilling the role of the endothecium, and a primary parietal layer generated a secretory tapetum and middle layer. Thus, we suggest that a new category of anther wall development, the *Arceuthobium* type, be created. Microsporogenesis produced tetrahedral microspores via simultaneous cytokinesis and involved callose wall formation. Microgametogenesis resulted in round and atypical generative and vegetative nuclei. Additionally, the heterocolpate, echinate pollen grains, which were shed at the two-celled stage, were seen for the first time in their native state with environmental scanning electron microscopy. This work contributes to the understanding of *A. americanum*, the genus *Arceuthobium*, and angiosperms as a whole.

Key words: anatomy, cytochemistry, dwarf mistletoe, microscopy, microsporogenesis, microgametogenesis.

Résumé : Le gui nain du pin lodgepole, *Arceuthobium americanum* Nutt. ex Engelm., est une angiosperme parasite qui infecte les conifères des forêts de l'Ouest du Canada. Alors que la production de pollen viable par les anthères est critique à la reproduction du gui nain, les rapports actuels, peu nombreux, qui se sont penchés sur le développement staminé chez *Arceuthobium* sont souvent incomplets ou contradictoires. L'objectif de ce travail était d'examiner l'anatomie développementale des anthères et du pollen d'*A. americanum* par microscopie moderne. Nous avons trouvé que le microsporange était en forme d'anneau dès le début et donnait naissance à une « columelle » centrale conoïde stérile tôt lors du développement de l'anthère. L'endothèque était absente, l'épiderme persistait comme « exothèque », remplissant le rôle de l'endothèque, et une couche pariétale primaire générait un tapetum sécrétoire et une couche intermédiaire; ainsi, nous suggérons qu'une nouvelle modalité de développement de la paroi de l'anthère soit créée, le type « *Arceuthobium* ». La microsporogénèse produisait des microspores tétraédriques par cytokinèse simultanée, et elle impliquait la formation d'une paroi calleuse. La microgamétogénèse résultait en noyaux génératifs et végétatifs ronds et atypiques. De plus, les grains de pollen hétérocolpés échinés qui étaient libérés au stade biloculaire ont été observés pour la première fois dans leur état natif par microscopie électronique à balayage environnemental. Ce travail contribue à mieux comprendre globalement *A. americanum*, le genre *Arceuthobium*, et les angiospermes.

Mots-clés : anatomie, cytochimie, gui nain, microscopie, microsporogénèse, microgamétogénèse.

Introduction

Dwarf mistletoes (genus *Arceuthobium*, Santalaceae) are obligate aerial parasites found on members of Pinaceae and Cupressaceae (Hawksworth and Wiens 1996). These dioecious parasites compromise the health of the host trees in North America, many of which are important timber species. Conifers infected with dwarf mistletoes show an overall reduction in growth, reproductive fitness, and wood quality, which equates to extensive product loss and, by extension, monetary losses to the lumber industry (Chhikara and Ross Friedman 2008; Hawksworth and Wiens 1996).

Arceuthobium americanum Nutt. ex Engelm. infects jack pine (*Pinus banksiana* Lamb.) in western Canada and lodgepole pine (*Pinus contorta* Douglas ex Loudan var. *latifolia* Engelm. ex S. Watson) in western North America (Godfree et al. 2002). The plant is a small yellowish to olive-green herbaceous angiosperm consisting of aerial shoots with whorled branching (Hawksworth and Wiens 1996)

connected to a network of cortical strands and radial sinkers that penetrate the coniferous host (Wilson and Calvin 1996). Being dioecious, the shoots from the individual plants will ultimately develop pistillate or staminate flowers. Pistillate flowers of *A. americanum* have two perianth parts, are bilaterally flattened and symmetrical, and have a heart-shaped dorsiventral face (Ross and Sumner 2004). The staminate flowers normally possess three sepals and no petals, with each sepal acting as a holding pad for a single sessile anther (Ross and Sumner 2004). Central to the sepals is a pad-like elevation of sterile tissue known as the central cushion, which secretes extremely sugary nectar (Penfield et al. 1976).

Production of viable pollen in anthers is critical to dwarf mistletoe reproduction and disease spread, yet only a handful of incomplete and often conflicting reports have examined development of the anthers and pollen in the staminate flowers. Regarding the *Arceuthobium* anther wall, authors generally agree that

Received 11 November 2013. Accepted 6 January 2014.

K.C. Munro, J.R.M. Jackson, I. Hartling, and C.M. Ross Friedman. Department of Biological Sciences, Thompson Rivers University, 900 McGill Road, Kamloops, BC V2C 0C8, Canada.

M.J. Sumner. Department of Biological Sciences, University of Manitoba, Winnipeg, MB R3T 2N2, Canada.

Corresponding author: Cynthia M. Ross Friedman (e-mail: cross@tru.ca).

the anthers lack a typical fibrously thickened endothecium and instead possess a persistent fibrously thickened epidermis (Bhandari 1984; Bhandari and Nanda 1968; Cohen 1968; Dowding 1931; Sereda 2003). Dowding (1931) used the term “exothecium” to describe this epidermis, whereas Bhandari and Nanda (1968) called it an “epithecium”. Largely because the epidermis persists, Cohen (1968), Bhandari (1984), and Sereda (2003) categorized the anther wall type in *Arceuthobium* as a modified form of the reduced type (Davis 1966). However, while no middle layer develops in the archetypical reduced type (Davis 1966), in *Arceuthobium* species, a uniseriate middle layer seems to develop from the primary parietal layer (Pisek 1924; Sereda 2003; Thoday and Johnson 1930). Cohen (1968) also described what is essentially a middle layer, even though he referred to it as the microsporangium wall. Whether or not this middle layer persists remains unclear. Regarding the tapetal wall layer, Sereda (2003) suggested that the *Arceuthobium* tapetum is uninucleate and secretory. Given the uncertainty of these data, a definitive description of anther wall development for *A. americanum* is needed.

While reports concur that the mature *Arceuthobium* microsporangium is unilocular, there is some disagreement as to its ontogeny and organization. Some authors have suggested that the sporangium is initially bisporangiate (Eichler 1875; Johnson 1888) or tetrasporangiate (Heinricher 1915; Staedter 1923) but that the partitions among the sporangia eventually break down, leading to the unilocular condition. Others (Bhandari and Nanda 1968; Bhandari and Vohra 1983; Cohen 1968; Pisek 1924; Sereda 2003; Thoday and Johnson 1930) concluded that the sporangium is unisporangiate upon initiation. Pisek (1924) further implied that, while unilocular, the mature sporangium has tapetal extensions that superficially resemble remnants of septae. Sereda (2003) also apparently observed tapetal extensions. As for its organization, various descriptions have suggested that the mature sporangium is ring shaped (Cohen 1968; Dowding 1931; Pisek 1924; Thoday and Johnson 1930), horseshoe shaped (Bhandari and Nanda 1968), or cup shaped (Sereda 2003), and that the sporangium, regardless of shape, encompasses a column of sterile tissue that Thoday and Johnson (1930) as well as Dowding (1931) called the “columella”. No author has convincingly demonstrated how this columella develops. Both Pisek (1924) and Dowding (1931) suggested that the orientation of the sporangium and columella is highly variable. Further complicating the matter, Bhandari and Vohra (1983) suggested that the horseshoe-shaped sporangium becomes ring shaped at maturity. Thus, the case for *A. americanum* needs further examination, and both the origin and final state of the columella needs clarification.

Similarly, only limited information can be found in the literature regarding microsporogenesis, microgametogenesis, and the mature pollen grain in *Arceuthobium*; electron microscopic investigations are unpublished. Bhandari and Vohra (1983) suggested that regular meiosis results in tetrahedral tetrads, and Sereda (2003) added that the microspores seem to form via simultaneous cytokinesis. Sereda (2003) also examined aspects of callose deposition but appeared to have problems with the fixation of some samples. Unequal cytokinesis in the *Arceuthobium* microspore has been said to lead to a lenticular-shaped generative cell and a large vegetative cell (Bhandari and Vohra 1983; Sereda 2003); mature pollen grains are apparently tricolpate, nearly spherical, shed at the two-celled stage, and spiny (Bhandari and Vohra 1983). However, detailed accounts of these processes and their timing along with characterizations of the microgametophyte are lacking.

Therefore, the objectives of this study were (1) to elucidate the processes of anther wall and pollen development in *A. americanum*, (2) to describe the eventual three-dimensional organization of the whole anther, and (3) to examine mature pollen in *A. americanum* using modern light and electron microscopy techniques. This information will further our knowledge of the life cycle of *A. americanum*

and may offer insights about the reproduction of these important forest pathogens.

Materials and methods

Site description, sample collection, and initial treatment of samples

Staminate *A. americanum* shoots with floral units (closed buds or open flowers) representing a range of developmental stages were collected twice weekly from 28 February 2011 to 30 June 2012. These samples were obtained from heavily infected lodgepole pine (*P. contorta* var. *latifolia*) trees located at a site adjacent to Stake Lake (50°31'N, 120°28'W), 30 km south of Kamloops, British Columbia. Fifteen randomly selected trees were flagged for repeated sampling from the same branch on the tree (1.5 m above the ground, as close to the trunk as possible) in an effort to regularly obtain shoots from the same *A. americanum* individual throughout the collection period and thus (ideally) minimize environmental variation. Without detailed genetic analysis, we cannot confirm whether or not aerial shoots of the same gender on an infected branch definitively belong to the same individual (i.e., result from the same infecting seed), and thus if the same individuals were always sampled in this study. Nonetheless, aerial shoots clustered together and emanating from the same regions of the branch most likely comprise the same individual (Chhikara and Ross Friedman 2008). Normally, two *A. americanum* shoots per tree (and ideally per individual *A. americanum*) were sampled each time for a total of about 250 shoots obtained over the entire collection period; each shoot contained at least 5 male floral units, and thus a total of about 1300 male floral buds or flowers were collected from the infected lodgepole pines.

To augment the data, about 100 additional staminate flowers that had previously been collected from infected *P. banksiana* in the Belair Provincial Forest (within 5 km of Belair, Manitoba, at 50°36'N, 96°32'W) biweekly from 1 May 1997 to 30 April 1998 were included in this study. Initial observations showed no differences in development between the sites, so all samples were analyzed collectively (also see Stewart and Ross 2006). All shoots and flowers were treated similarly for the rest of the study.

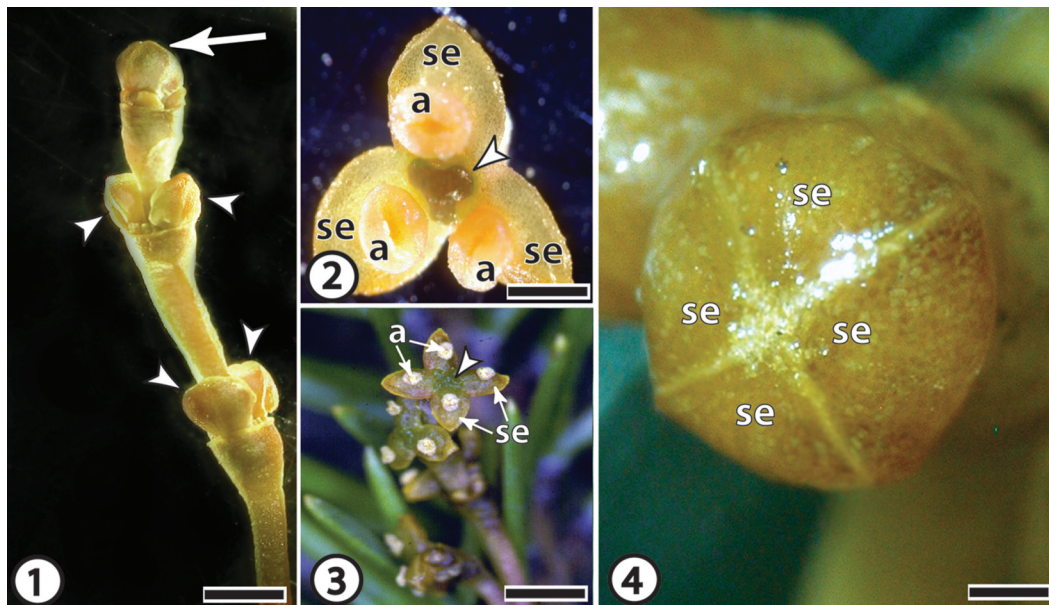
In the field, most shoots were placed in a fixative consisting of 2% (*m/v*) paraformaldehyde + 2% (*m/v*) glutaraldehyde in 0.1 mol·L⁻¹ phosphate buffer (pH 6.8), although a few randomly selected shoots collected in British Columbia were not fixed onsite but were instead taken back to the laboratory for immediate examination under a Nikon SMZ 1500 dissecting microscope equipped with a Nikon Coolpix 995 camera (Nikon, Tokyo, Japan). Additionally, some unprocessed shoots with open flowers obtained in May and June of 2012 were shaken over carbon-tape-covered scanning electron microscopy (SEM) stubs to capture mature pollen grains, which were immediately viewed in their native state (no fixation, no sputter coating) with a Zeiss LS15 Evo SEM (Carl Zeiss Microscopy Ltd., Cambridge, UK) operating in Extended Pressure mode with air (45 Pa pressure).

Shoots in fixative were returned to the laboratory, kept at 4 °C overnight, then rinsed in the same buffer. Individual staminate floral buds or flowers were excised and postfixed with 2% (*m/v*) osmium tetroxide in the same buffer for 4 h. All fixed material was then dehydrated in an ethanol to propylene oxide series and embedded in Spurr's epoxy resin (Spurr 1969).

Bright-field and fluorescence light microscopy

From each Spurr's-resin-embedded male bud or flower, 8 sections (1 median and 7 nearly median × 5 floral units, for a total of 5 median and 35 nearly median sections per date) of 2 μm thickness were obtained with a Sorvall MT2-B ultramicrotome (Thermo Fisher Scientific, Waltham, Massachusetts, USA) and affixed to Superfrost® Plus Gold Slides (Electron Microscopy Sciences, Hatfield, Pennsylvania, USA). About half of these slides (including

Figs. 1–4. Organization and general morphology of staminate inflorescences and their floral units (buds or open flowers) of *Arceuthobium americanum*. **Fig. 1.** General organization of the inflorescence (sampled just prior to anthesis, 1 April 2011). Decussately arranged buds (arrowheads) are found below the terminal one (arrow). Scale bar = 5 mm. **Fig. 2.** Mature and open staminate trimerous *A. americanum* flower possessing a dark-green trilobed central cushion and nectary (arrowhead), surrounded by a whorl of three yellowish green sepals (se), each bearing a single sessile, pale yellow anther (a) (sampled during anthesis, 20 May 2011). Scale bar = 1 mm. **Fig. 3.** Tetramerous *A. americanum* staminate flower at anthesis, arrowhead indicates nectary (sampled 20 May 2011). a, anther; se, sepal. Scale bar = 5 mm. **Fig. 4.** Tetramerous *A. americanum* staminate bud (sampled just prior to anthesis, 1 April 2011). se, sepal. Scale bar = 250 μ m.



those with median sections) were stained with 2% (*m/v*) crystal violet in a 0.05 mol·L⁻¹ ammonium oxalate buffer (pH 6.7) — a stain we felt worked well with Spurr's resin — and viewed with a Nikon Eclipse E400 light microscope (Nikon, Tokyo, Japan). Spurr's resin was extracted from the remaining slides using the method outlined by Sutherland and McCully (1976). Most of the slides with resin-free sections were stained with 0.05% Aniline Blue (*m/v*) in a 0.01 mol·L⁻¹ phosphate buffer (pH 6.8) for the detection of callose (O'Brien and McCully 1981) and were observed with the Nikon E400 microscope fitted with a Nikon episcopic fluorescence attachment and an excitation filter transmitting 410–485 nm. About 10 unstained resin-free sections containing microspores were observed with the same microscope fitted with the fluorescence attachment and an excitation filter transmitting 540–580 nm to detect autofluorescence from sporopollenin (Willemse 1972). Slides were photographed with a Nikon E995 3.34 mp camera. In all cases, photographs were obtained with the Nikon E995 3.34 mp camera (Nikon, Tokyo, Japan).

Transmission electron microscopy (TEM)

For TEM, about 5 ultrathin sections of 50–100 nm in thickness (grey to gold interference colours) were obtained from each Spurr's-resin-embedded flower or bud (5 sections × 5 floral units per date) with the Sorvall MT2-B ultramicrotome and adhered to the shiny side of uncoated copper hex grids (200 mesh). The sections were stained with saturated uranyl acetate in 50% methanol and counterstained with 0.1% aqueous lead citrate. All sections were observed with a Zeiss TEM (Carl Zeiss Microimaging Inc., Thornwood, New York, USA) at an operating voltage of 60 kV. Images were digitized with a Hamamatsu ORCA-HR C4742-95-12HR C4742-95 Digital CCD Camera (Hamamatsu Photonics K.K., Hamamatsu, Japan).

Results

Overview and orientation of the mature staminate inflorescences and flowers

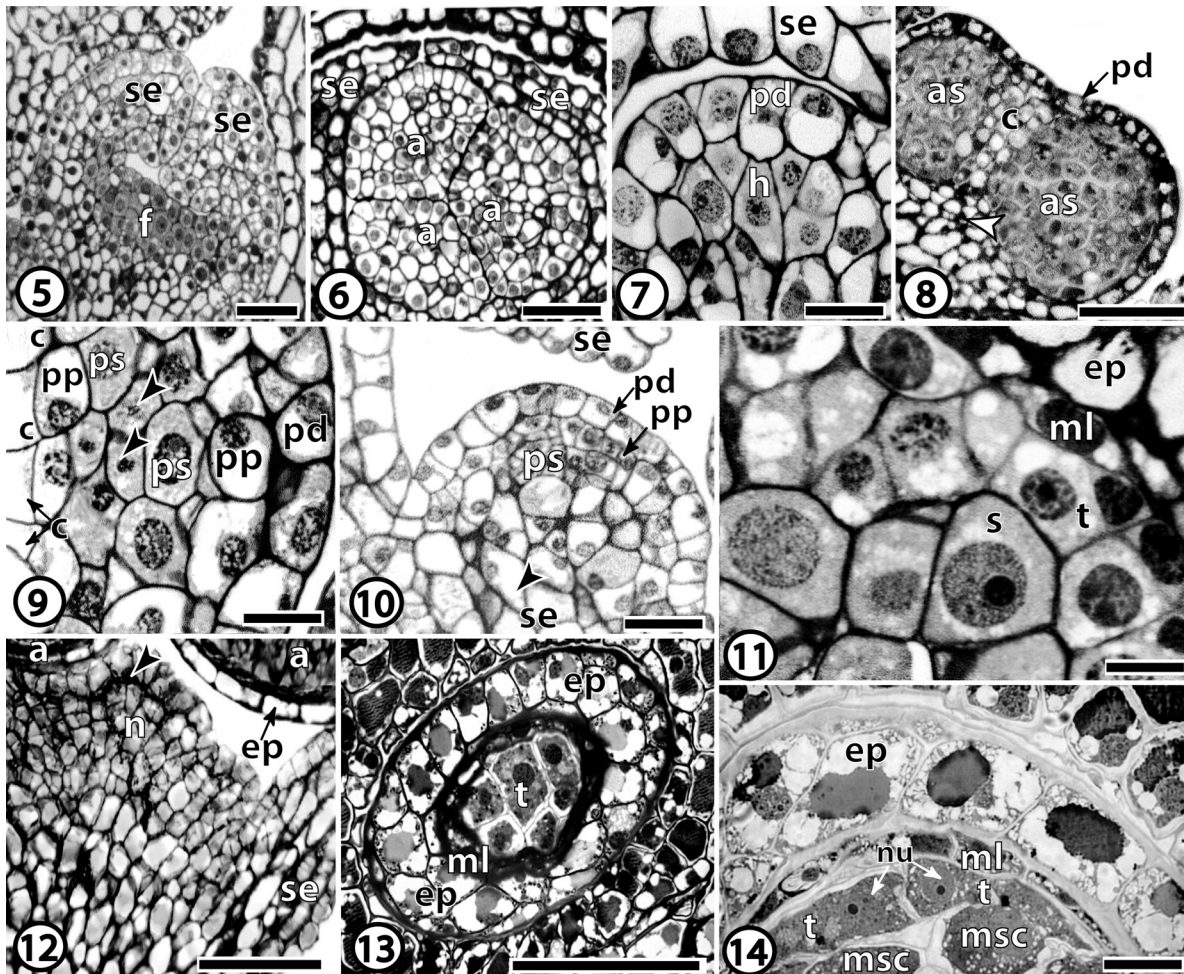
Staminate inflorescences of *A. americanum* consist of a single terminal floral unit (closed bud or open flower) with two oppo-

sitely arranged lateral floral units positioned immediately below the terminal one (Fig. 1). Longer stems possess additional sets of floral units below the laterals, arranged decussately, and whole aerial shoots often have decussately branched lateral stems. A mature staminate *A. americanum* flower has a dark-green lobed central cushion (nectary) surrounded by a whorl of yellowish green sepals, each sepal bearing a single sessile, pale yellow anther (Fig. 2). In this study, we examined about 1300 staminate flowers at different stages of development from what we assumed to be 15 different individuals in British Columbia, and we can conclude that the staminate flowers are normally trimerous (about 80% ± 5% of the flowers) but occasionally (20% ± 5%) tetramerous (Figs. 3 and 4), with the distribution of types being the same within and among different individuals. We observed only two dimerous staminate flowers (not shown). The central cushion typically has the same number of lobes as sepals; the lobes alternate with the sepals (Fig. 2). The sepals are "rowboat shaped" in outline and are yellowish green, whereas the anthers are oval (as they are slightly elongated in their transverse axis perpendicular to the long axis of a sepal) and pale yellow. The stamens never develop vascular supplies that are independent from those of the sepals.

Anther initiation: sporogenous tissue, columella, and anther wall

In British Columbia, fully mature staminate flowers shed pollen and abscise in the late spring (mid-May to early June). When a flower abscises, a young meristem is revealed and immediately resumes floral development, forming sepal primordia to enclose the young floral axis (Fig. 5). Each staminate bud will ultimately produce another flower that will become wholly mature the following spring. In a newly forming staminate bud, the (normally) three stamen (anther) primordia become evident in mid-June as closely appressed mounds of tissue that originate at the floral apex and are contained in the sepals (Fig. 6). Floral development is somewhat advanced in the apical regions of the inflorescence, with the terminal bud being the furthest ahead in development,

Figs. 5–14. Origin of the anther wall and development of the sporogenous tissue. **Figs. 5–7.** Development in a newly forming bud (sampled 1 June 2011) following anthesis. **Fig. 5.** Longitudinal section of a young floral apex (f) and two of the three sepal primordia (se). Scale bar = 100 μm . **Fig. 6.** Cross-section of the three incipient anther primordia (a) contained within the sepals (se); only two of three sepals are shown. Scale bar = 50 μm . **Fig. 7.** Longitudinal section through an incipient anther, revealing the uniseriate protoderm (pd) surrounding several layers of densely cytoplasmic and meristematic hypodermal cells (h). se, sepal. Scale bar = 20 μm . **Fig. 8.** Median longitudinal section of an anther showing development of the columella (c) within the anther (sampled 20 June 2011). The columella stretches from the anther's base (arrowhead) to its apex, where the columella becomes continuous with the protoderm (pd). A torus of archesporial cells (as) surrounds the columella. Scale bar = 100 μm . **Figs. 9 and 10.** Production of the primary parietal and the primary sporogenous layer (sampled 29 June 2011). **Fig. 9.** Nonmedian longitudinal section of the anther where cells of the outermost archesporial layer in contact with the protoderm (pd) and the columella (c) have produced the uniseriate primary parietal (pp) layer toward the outer and inner periphery of the torus, and the primary sporogenous (ps) layer away from the periphery. The remaining deeply located archesporial cells act directly as sporogenous tissue (arrowheads). Scale bar = 25 μm . **Fig. 10.** Conjoining of the basal portion of the anther with the sepal (se) through a common belt of tissue (arrowhead) that results from intercalary meristematic activity. pd, protoderm; pp, primary parietal layer; ps, primary sporogenous tissue. Scale bar = 40 μm . **Figs. 11–13.** Production of the middle layer and tapetum (sampled 5 July 2011). **Fig. 11.** Uniseriate middle layer (ml) in contact with the epidermis (ep) matured from protoderm, and uniseriate tapetum (t) in contact with the sporogenous cells (s). Scale bar = 10 μm . **Fig. 12.** Longitudinal section of the central cushion or nectary (n) at the centre of the flower. Accumulations of darkly staining material, possibly secreted, are indicated by an arrowhead. a, anther; ep, epidermis; se, sepal. Scale bar = 100 μm . **Fig. 13.** Glancing section of an anther's surface, capturing the surface of the tapetum (t) and partial surfaces of the middle layer (ml) and epidermis (ep). Scale bar = 100 μm . **Fig. 14.** Sporogenous cell divisions cease, and by mid-August (here 14 August 2011), the cells have matured into microsporocytes (msc). The tapetum (t) is uninucleate and cytoplasmic. ep, epidermis; ml, middle layer; nu, nuclei. Scale bar = 20 μm .



often a day or so in advance of the lowermost flowers (not shown). Each incipient anther consists of a uniseriate protoderm surrounding several layers of meristematic, densely cytoplasmic hypodermal cells (Fig. 7). By late June, a column of parenchymatous cells that are centrally located in the hypodermal mass becomes highly vacuolate, and the nuclei in the cells of this column or "columella" become less prominent (Fig. 8). The columella stretches from the anther's base to its apex, where cells of the columella's peltate "head" become continuous with the proto-

derm. The remaining hypodermal cells completely surround the columella as a torus of archesporial cells. Different planes of section would erroneously indicate that this columella is branched and that the archesporium is oval or horseshoe shaped. However, serial sectioning and examinations with the dissecting microscope revealed that the columella is like a peg in the continuous donut-shaped archesporial region. We had difficulty obtaining long sections because the anthers are obliquely positioned on the floral axis and somewhat twisted. The most accurate way to de-

scribe the true median section is to say that it has a “butterfly” appearance, with the columella forming the body, and the archesporium the wings of the butterfly (Fig. 8).

By the end of June, cells of the outermost archesporial layer, which contact the protoderm on the outer face of the torus and the columella on the inner face of the torus, asynchronously undergo periclinal divisions to produce (1) the primary parietal layer toward the outer periphery of the torus and (2) the primary sporogenous layer away from the periphery (Fig. 9). As a result, the primary parietal layer lines the protoderm and the columella. The remaining deeply located archesporial cells continue to divide mitotically, acting directly as primary sporogenous tissue. These cells fit together tightly and are polygonal to oval in shape. At this time, the basal portion of the anther conjoins with the sepal through a common belt of tissue that results from intercalary meristematic activity, and thus, each anther soon becomes fused to a sepal (Fig. 10).

In early July, the cells of the primary parietal layer divide periclinally once again to form a uniseriate middle layer at the periphery (in contact with the protoderm or columella) and a vacuolate uniseriate tapetum away from the periphery; this tapetum maintains contact with the sporogenous cells (Fig. 11). Because of its central position and the accumulation of darkly staining material among its cells (likely secreted), a well-developed nectary can be identified in the flower at this time (Fig. 12). The protoderm, the cells of which have become quite vacuolate and radially elongated, has matured into a uniseriate epidermis (Figs. 11–13). While some planes of section seem to show that the tapetum, middle layer, and epidermis are more than one cell layer thick (Fig. 13), especially at the anther base (not shown), this appearance is partially a function of sectioning into the layer itself and (or) sectioning into the parenchymatous cells of the columella; it is also due in part to the intercalary activity at the base of the anther (Fig. 10).

The sporogenous cells continue to divide mitotically into mid-August. When these divisions cease, the anther has reached its largest size, and the sporogenous cells can now be referred to as microsporocytes or microspore mother cells. At this time, the anther possesses a highly vacuolate epidermis surrounding the smaller flattened cells of the middle layer, which in turn surround a uninucleate, cytoplasmic tapetum (Fig. 14). The cells of the columella remain vacuolate, are lined by the middle layer, and are continuous with the epidermis (not shown).

Microsporogenesis and continued anther wall development

The anther reaches its maximum size in mid-August. At this time, the microsporocytes enter prophase I of meiosis (Fig. 15). Intercellular spaces appear among individual microsporocytes and between the microsporocytes and the anther wall. These spaces develop because the microsporocytes begin to pull away from each other as they “round up” and also because the loculus expands at the expense of the middle layer. The epidermis remains firmly attached to the head of the columella, while the toroidal loculus encircling the columella swells (Fig. 16). Although the middle layer is becoming crushed, it still possesses intact nuclei and cell walls (Fig. 15). Tapetal cells remain highly cytoplasmic. In cross-section (face view), the anther appears to be oval, with the long transverse axis of the oval arranged perpendicularly to the long axis of the sepal (Fig. 17). The head of the columella has become slightly elongated in the anther’s long transverse axis as well. Adjacent microsporocytes do maintain some contact with each other, and individual microsporocytes retain their cell walls (Figs. 15 and 18). As previously, the middle layer and tapetum lines the columella (Fig. 17). Adjacent microsporocytes do maintain some contact with each other, and individual microsporocytes retain their cell walls (Figs. 15 and 18). Cytomictic channels can be seen between tapetal cells; these cells take on an irregular shape (Fig. 19). Apparently, however, no cytomictic channels connect the microsporocytes to the tapetal cells.

By about the third week in August, the microsporocytes, still in early meiosis I, have become even rounder and the spaces among them more prominent (Fig. 20). Their cell walls also become considerably thicker due to impregnation with callose (Figs. 20–22), and cytomictic channels as large as 0.6 μm in diameter can be observed in the regions where two microsporocytes contact each other (Fig. 22). The callose accumulates between the plasma membrane and the original microsporocyte cell wall. Completion of meiosis I leads to the formation of a binucleate dyad (Fig. 23), and the two nuclei of the dyad rapidly undergo meiosis II (likely within hours) to form four nuclei (Fig. 24). The nuclear divisions are immediately followed by a simultaneous cytokinesis to produce a tetrad of tetrahedrally arranged haploid microspores (Fig. 25). Each microspore in a tetrad is encased in an Aniline-Blue-positive callose cell wall (Fig. 26).

Free microspores

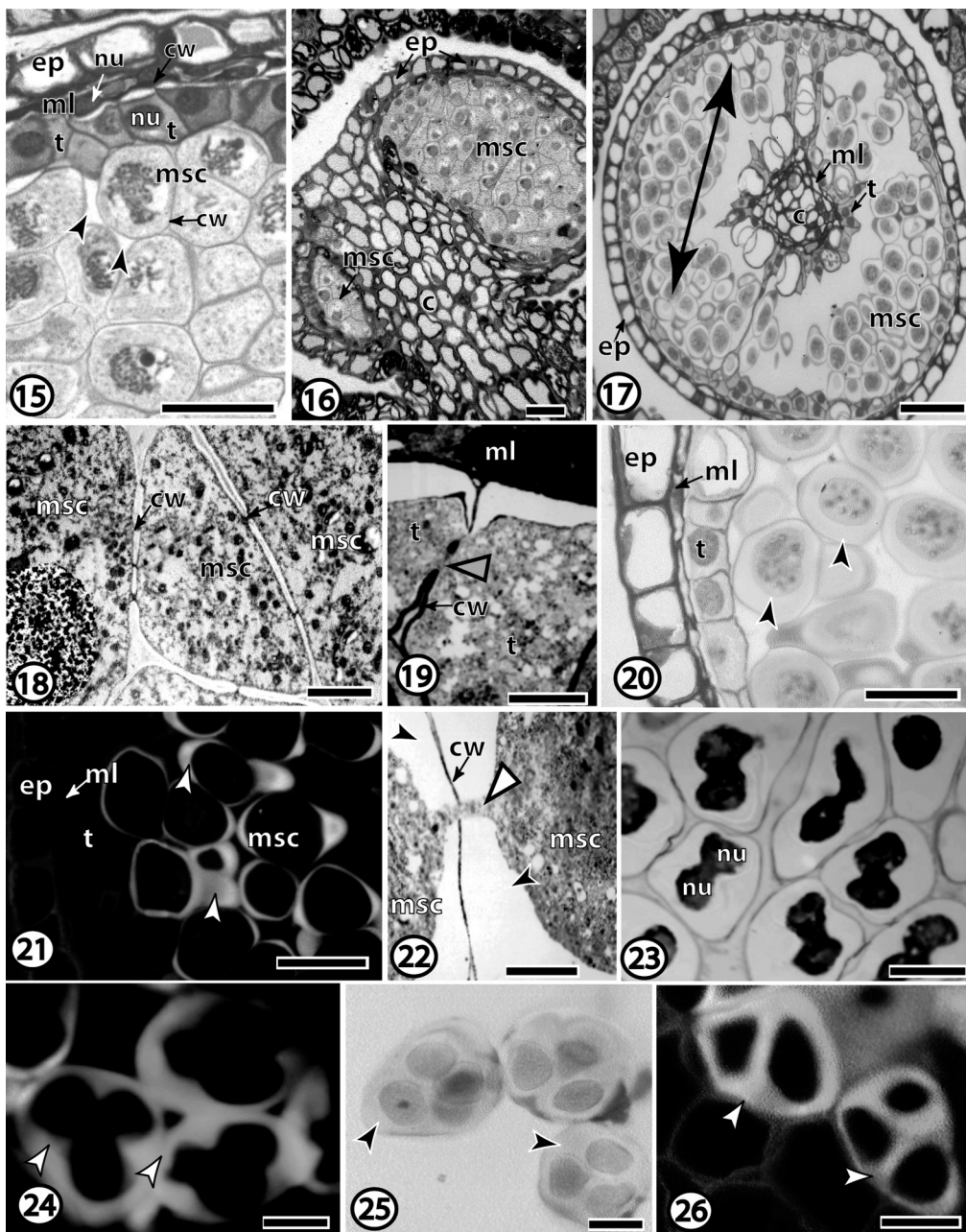
By the last week in August, the callose wall disappears, and the microspores, which are about 9 μm in diameter, detach from each other and become separated by 5–9 μm spaces (Fig. 27). They are somewhat misshapen relative to the round shape they will soon develop, as they retain some of the configuration of the tetrad. Each microspore has developed a relatively thin external cell wall that autofluoresces (not shown), suggestive of an exine that contains sporopollenin. At this time, the tapetum shows evidence of secretory activity (Fig. 28; e.g., endoplasmic reticulum stacks), while the middle layer persists (Figs. 27 and 28). The tapetum stains darkly, which suggests it might be undergoing programmed cell death. Cells of the epidermis, however, become further radially elongated and develop thin (about 3 μm), fibrous bands along their inner tangential walls (Figs. 27 and 29). The fibrous bands run up all four radial cell walls, coming to an end near the outer tangential wall of each epidermal cell.

Microspore maturation, microgametogenesis, and the maturing anther wall

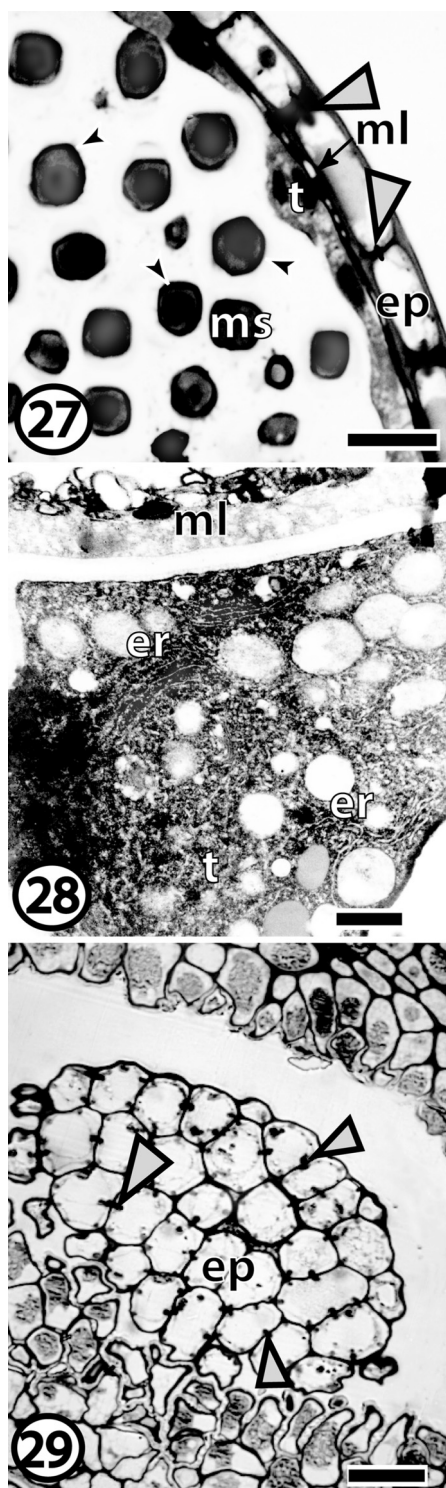
At the end of August, prior to microgametogenesis, the microspores rapidly increase in size, reaching 20–25 μm in diameter, which is more than double their original size upon release from the tetrads (Fig. 30). The microspore cell walls autofluoresce strongly when illuminated with 540–580 nm light, indicating the presence of sporopollenin (Fig. 31). Examination with TEM shows that the microspores possess a distinctly stratified cell wall composed of an inner cellulosic intine and an outer sporopollenin-rich exine; they also have three true colpi (apertures) that alternate with three pseudocolpi (Fig. 32). These six grooves give the pollen an undulating border when viewed in cross-section. The intine at each colpus is thickened, and the exine is thinned. However, at the pseudocolpi, as well as the remaining pollen surface, the intine and exine are uniformly thickened. The single nucleus of each microspore remains centrally located (Figs. 30 and 32). The uninucleate cells of the tapetum have developed warped, indistinct boundaries (Fig. 30). The inner surface of the tapetum possesses many osmiophilic orbicules (Fig. 33).

Initiation of microgametogenesis occurs at the beginning of September, when the first mitotic division of the microspores occurs. As mitosis completes, a central cell plate will develop between the two resultant similar-sized nuclei, which are equidistant from each other and from the immature pollen grain cell wall (Fig. 34). The mitosis is more or less synchronous, but perhaps not perfectly so, as the occasional undivided microspore could still be seen. Within a day or two, the cell wall will curve around one of the nuclei (the generative nucleus) and fuse with the now bilayered intine to form the generative cell (Figs. 35 and 36). The generative cell is subsequently freed from the intine by the constriction of the generative cell wall between its nucleus and the intine. At this point, the entire generative cell is almost entirely composed of nuclear material; the generative nucleus

Figs. 15–26. Microsporogenesis and accompanying changes in the anther. **Figs. 15–19.** Microsporocytes begin prophase I (15 August 2011). **Fig. 15.** Spaces (arrowheads) among the microsporocytes (msc). The uninucleate tapetum (t) is densely cytoplasmic. ep, epidermis; cw, cell wall; nu, nucleus; ml, middle layer. Scale bar = 20 μm . **Fig. 16.** Near-median longitudinal section of the anther featuring the columella (c), whose head remains attached to the epidermis (ep). msc, microsporocytes. Scale bar = 20 μm . **Fig. 17.** Cross-section taken near the top of the anther. The head of the columella (c) has become slightly elongated in the anther's long transverse axis, which is indicated by the double-headed arrow. The middle layer (ml) and tapetum (t) line the columella. ep, epidermis. Scale bar = 60 μm . **Figures 18 and 19** are transmission electron micrographs (TEM). **Fig. 18.** Typical cellulose cell walls (cw) surrounding the microsporocytes (msc). Scale bar = 5 μm . **Fig. 19.** Cytomictic channel (large open arrowhead) between adjacent tapetal (t) cells. cw, cell wall; ml, middle layer. Scale bar = 10 μm . **Figs. 20–22.** Cell wall thickening during microsporogenesis (17 August 2011). **Fig. 20.** Late prophase I microsporocytes with thickened cell walls (arrowheads). ep, epidermis; ml, middle layer; t, tapetum. Scale bar = 20 μm . **Fig. 21.** Similar section as that in **Fig. 20**, stained with Aniline Blue. Thickened walls (arrowheads) fluoresce due to the likely presence of callose. ep, epidermis; ml, middle layer; msc, microsporocytes; t, tapetum. Scale bar = 20 μm . **Fig. 22.** TEM of cytomictic channels (large open arrowhead) connecting adjacent microsporocytes (msc) through the callosic cell wall (cw) (small closed arrowheads). No cytomictic channels link the microsporocytes to the tapetum. Scale bar = 2 μm . **Fig. 23.** Dyads with two nuclei (nu) forming as meiosis I concludes (19 August 2011). Scale bar = 10 μm . **Fig. 24.** Aniline-Blue-stained section of tetrads containing four haploid microspores (the fourth is out of the plane of section) captured prior to complete cytokinesis (19 August 2011). The thickened cell walls likely contain callose, as they fluoresce (arrowheads). Scale bar = 20 μm . **Figs. 25–26.** Tetrads following cytokinesis (sampled 22 August 2011). **Fig. 25.** Tetrahedral arrangement of the microspore tetrads encased in thick cell walls (arrowheads). Scale bar = 20 μm . **Fig. 26.** Aniline-Blue-stained section similar to that in **Fig. 25**, revealing thickened fluorescent cell walls (arrowheads) likely containing callose. Scale bar = 20 μm .



Figs. 27–29. Separation of the microspores and further changes in the anther wall (sampled 26 August 2011). **Fig. 27.** Free uninucleate microspores (ms) with thin outer walls, likely infused with sporopollenin (small closed arrowheads). Radial thickenings (large open arrowheads) can be seen in the epidermis (ep). ml, middle layer; t, tapetum. Scale bar = 20 μm . **Fig. 28.** Transmission electron micrograph showing darkly staining tapetal cells (t) containing endoplasmic reticulum (er). Scale bar = 2 μm . **Fig. 29.** Glancing section of the anther epidermis (ep) showing the radial fibrous thickenings “head on” (large open arrowheads). Scale bar = 50 μm .



remains central and rounded throughout this entire process. Meanwhile, the vegetative nucleus, housed within the original boundary of the microspore, takes on a lenticular appearance and soon partially envelops the generative cell like a shallow cup. The tapetum is broken down, and the middle layer has finally been obliterated and is now only a crushed remnant (**Fig. 36**).

By mid-September, the staminate floral buds reach the stage at which they will overwinter. The sepals still tightly enclose the anther, where the epidermis with fibrous thickenings is the only remaining layer of the anther wall (**Fig. 37**). The pollen grains, which remain encased within the epidermal layer, have walls composed of a spiny exine and a thick, underlying bilayered intine (**Fig. 38**). On its outer surface, the exine is coated with electron-opaque material, likely pollenkitt; similar materials are also seen in the loculus and often connect pollen grains to each other. The generative cell has undergone an enlargement and possesses horn-like cytoplasmic extensions, although its nucleus remains rounded in shape (**Figs. 38 and 39**). The microgametophytes overwinter in the closed flowers and anthers as bicellular pollen grains and will ultimately be released at this stage of development the following spring. Similarly, no further changes in the flower or anther occur until the following spring.

Anthesis, mature pollen, and pollen dispersal

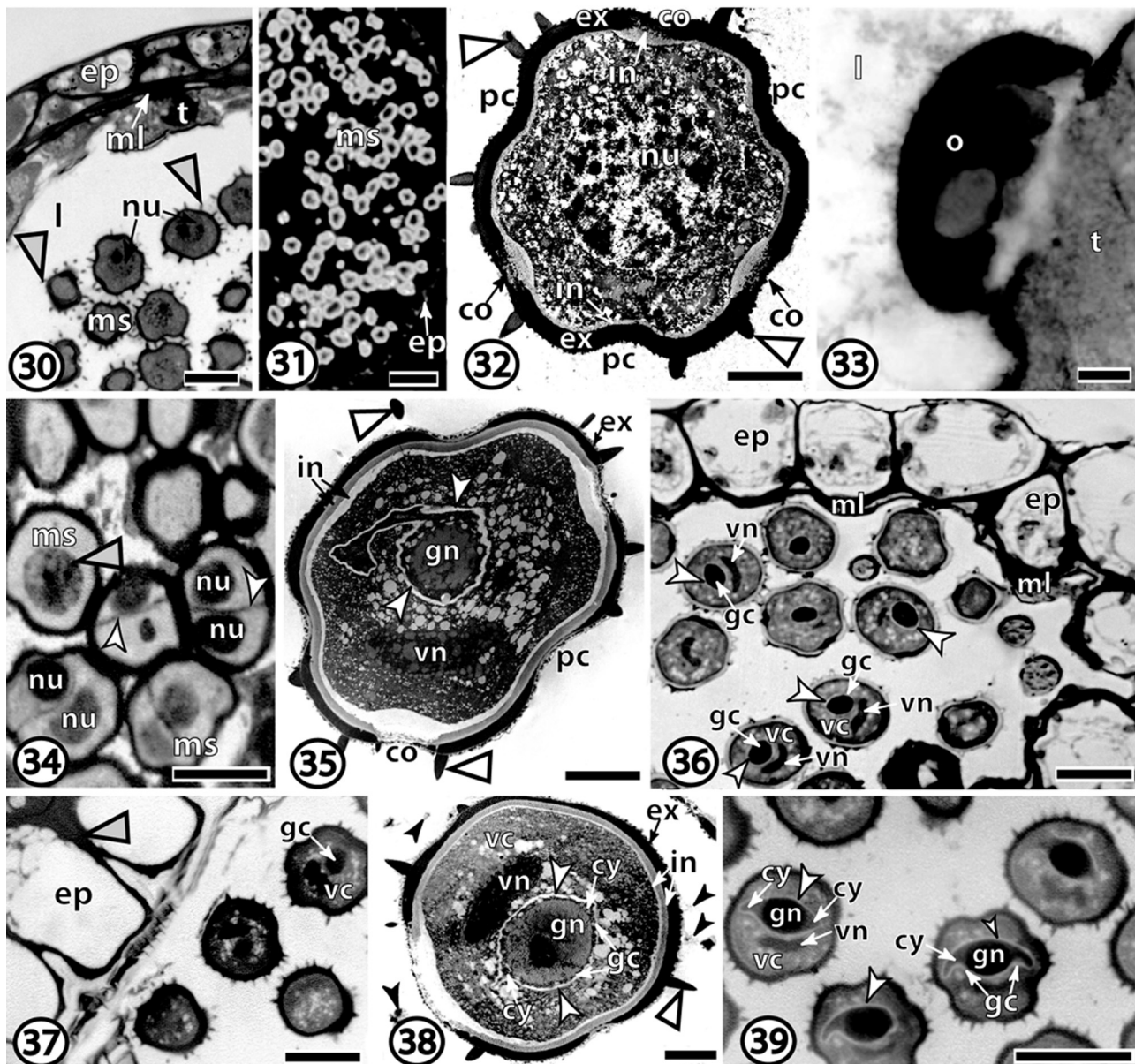
In mid-May of the year following anther initiation, the flowers undergo asynchronous anthesis over the subsequent three to four weeks to slowly release mature yellow-coloured pollen (**Fig. 40**) at the two-celled stage (unchanged from **Figs. 38 and 39**). For pollen dispersal, a slit forms on the upper surface of the anther (**Fig. 40**). The slit is perpendicular (transverse) to the long axis of the sepal but parallel to the longer transverse axis of the oval anther itself. To form the slit, a central region of the fibrously thickened epidermal cells in contact with the elongated head of the columella forms a central groove and seems to degenerate along with a few of the uppermost cells of the columella. The resultant slit mirrors the shape and orientation of the underlying head of the columella and opens to enable pollen dispersal. Although initial dispersal of pollen is somewhat explosive, not all of the pollen is released at this time. The surface of the pollen exine is textured (**Figs. 41 and 42**) and covered by persistent pollenkitt (**Fig. 41**), which would bond remaining pollen grains to the columella and glue dispersed pollen grains together in clumps (**Fig. 40**). The dispersed pollen is shaped like a prolate spheroid, with the shorter equatorial diameter being about 24 μm and the longer polar diameter averaging 6 μm larger (**Fig. 42**). The spines of the echinate grains vary in height from about 1 to 3 μm . The three colpi extend from pole to pole and alternate with the three pseudocolpi, which are shorter. These six indentations are equidistant from one another around the circumference of the grain.

Discussion

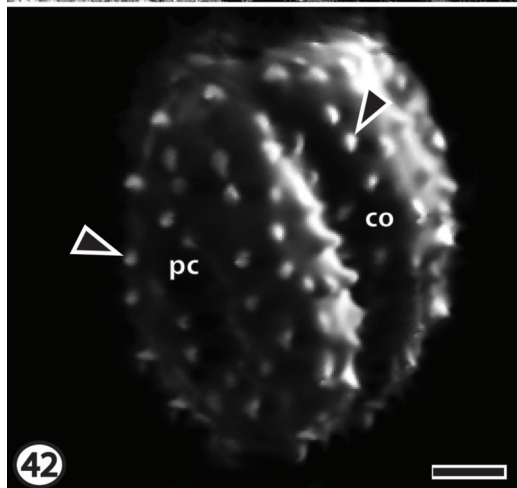
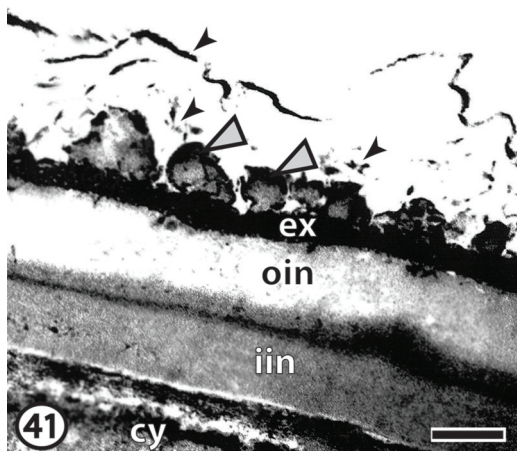
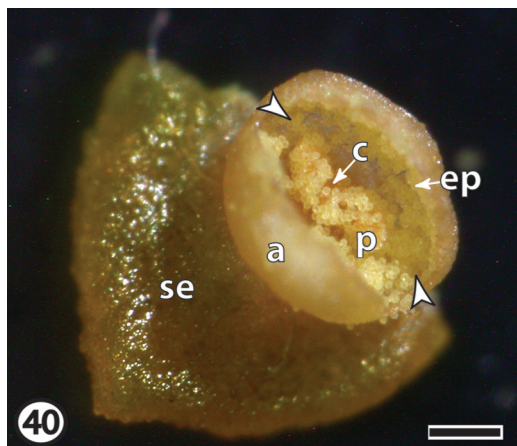
Organization of the mature flower

The perianth segments of the staminate flowers in *Arceuthobium* have been called sepals (**Cohen 1968**), tepals (**Polhill and Wiens 1999**), perianth parts (**Sereda 2003**), and petals (**Heide-Jørgensen 2008**). We elected to call the perianth segments “sepals” because of their role in protecting the anthers during development and because of **Cohen’s (1968)** convincing illustrations of sepal-like initiation. Regardless of what the perianth parts are called, there were normally three of them, although there were occasionally four and rarely two. Our data generally concur with those of others (**Cohen 1968; Dowding 1931; Sereda 2003**), although these authors’ results indicated that dimerous flowers occurred more often than we observed. It is difficult to make direct comparisons, however, as those authors did not attempt to quantify the frequency of flower types.

Figs. 30–39. Microspore development, microgametogenesis, and anther wall maturation. **Figs. 30–33.** Expansion of the uninucleate microspores (sampled 29 August 2011). **Fig. 30.** Enlarged microspores (ms), each with a centrally located nucleus (nu). Large open arrowheads indicate spikes. Cells of the tapetum (t) no longer have discrete boundaries. ep, epidermis; l, loculus; ml, middle layer. Scale bar = 20 μm . **Fig. 31.** Autofluorescence of the microspores (ms) excited by 540–580 nm light. ep, epidermis. Scale bar = 60 μm . **Fig. 32.** Transmission electron micrograph (TEM) of a microspore with its central nucleus (nu). The cell wall is stratified, possessing an exine (ex) and an intine (in). Three colpi (co) alternate with three pseudocolpi (pc). Large open arrowheads indicate spikes. Scale bar = 5 μm . **Fig. 33.** TEM of the tapetum (t) showing an osmiophilic orbicule (o). Scale bar = 500 nm. **Figs. 34–37.** Initiation of microgametogenesis (sampled 2–4 September 2011). **Fig. 34.** Nascent cell plate (small arrowheads) formation in each microspore (ms) after the first mitosis (2 September 2011), separating the two nuclei (nu). The odd microspore has not divided (large open arrowhead). Scale bar = 20 μm . **Fig. 35.** TEM of a microspore (sampled 4 September 2011), a few days following that in **Fig. 34**. The cell plate, now a cell wall (small open arrowheads) curving around the central rounded generative nucleus (gn) to form the generative cell, has begun to encroach upon the original microspore wall. The vegetative nucleus (vn), housed in the original microspore confines to form the vegetative cell, is lenticular. Large open arrowheads indicate spikes. The intine (in) now appears bilayered. co, colpi; ex, extine; pc, pseudocolpi. Scale bar = 5 μm . **Fig. 36.** Centrally located generative cell (gc), which is essentially entirely nuclear, with its enveloping cell wall (open arrowheads). The tapetum has degenerated and can no longer be discerned, and the middle layer (ml) has been obliterated into a crushed remnant. ep, epidermis; vc, vegetative cell; vn, vegetative nucleus. Scale bar = 20 μm . **Figs. 37–39.** Appearance of the pollen grains prior to overwintering (sampled 15 September 2011). **Fig. 37.** Epidermis (ep) with fibrous thickenings (large open arrowheads) is the only remaining anther wall. gc, generative cell; vc, vegetative cell. Scale bar = 25 μm . **Fig. 38.** TEM of the bicellular pollen grain with its exine (ex) and bilayered intine (in). Large open arrowheads indicate spikes. Granular electron-opaque materials, likely pollenkit (small closed arrowheads), line the exine's surface and are also found in the loculus (l). The generative cell (gc) possesses horn-like cytoplasmic extensions (cy), although its nucleus (gn) remains rounded. Small open arrowheads indicate the generative cell wall. vc, vegetative cell; vn, vegetative nucleus. Scale bar = 5 μm . **Fig. 39.** Light-level image showcasing the round generative nucleus (gn) and cytoplasmic extensions (cy) of the generative cell (gc) in the bicellular microgametophyte. Open arrowheads indicate the generative cell wall. Scale bar = 25 μm .



Figs. 40–42. The anther and its pollen at anthesis (sampled the following spring, 16 May 2012). **Fig. 40.** One sepal (se) with its anther (a) containing yellow pollen (p). A slit (arrowhead) transverse to the long axis of the sepal forms in the epidermal cells (ep). Pollen in clumps adheres to the columella (c). Scale bar = 330 μm . **Fig. 41.** A transmission electron microscopy section showing that the surface of the dispersing pollen exine (ex) is textured (large open arrowheads) and covered by persistent electron-opaque pollenkitt (small closed arrowheads). The two layers of the intine, the outer intine (oin) and the inner intine (iin), are evident. cy, cytoplasm. Scale bar = 500 nm. **Fig. 42.** Scanning electron micrograph of dispersed pollen shaped like a prolate spheroid. Arrowheads indicate the spines. co, colpi; pc, pseudocolpi. Scale bar = 6 μm .



Initiation of the anther and development of anther wall, sporogenous tissue, and columella

Eichler (1875) speculated that because of their intimate connection, the sepals and stamens comprised one phyllome. However, we found that the sepals developed separately from, and prior to, development of the anthers, which only become conjoined to the surface of the sepals following intercalary growth. Thus, our findings support those of Johnson (1888) and Sereda (2003), who proposed that the sepals and stamens do not emanate from the same phyllome.

Our description of the development of the anther wall layers generally agrees with those provided in other studies of *Arceuthobium* (Bhandari 1984; Bhandari and Nanda 1968; Cohen 1968; Dowding 1931; Pisek 1924; Thoday and Johnson 1930; Sereda 2003). As in these other studies, we found that the epidermis persisted as a fibrously thickened region (exothecium), an endothecium did not develop, and a primary parietal layer gave rise to a uniseriate tapetum and middle layer. However, we found that the middle layer persisted longer than had been described in other *Arceuthobium* studies (Cohen 1968; Sereda 2003), remaining obvious even when bicellular pollen was present in the anther. Nonetheless, is not uncommon for the timing of middle layer degeneration to differ among angiosperms and for degeneration to be delayed until microgametogenesis occurs (Anjaneyulu and Lakshminarayana 1989). As is true for many angiosperms, cells of the middle layer in *A. americanum* did not undergo anticlinal divisions, although they seemed particularly capable of being stretched. In addition, the serial sectioning we carried out demonstrated that the tapetum was uninucleate, although other genera closely related to *Arceuthobium* within the family Santalaceae (ascribed to the former family Viscaceae) have bi- or tetranucleate tapetal cells (Davis 1966). We also did not observe the tapetal extensions seen by Pisek (1924) and Sereda (2003), and suggest that their observations of extensions resulted from sectioning into the tapetal surface. Like Sereda (2003), though, we believe that the tapetum is of the secretory type, since the tapetum released orbicules, the small sporopollenin bodies associated with secretory tapeta (Gonzalez et al. 2001; Shukla et al. 1998).

It is also important to note that because the columella arises early in development, anther wall layer development is more complicated than described in the earlier studies: the primary parietal layer not only initiates adjacent to the protoderm but also adjacent to the nascent columella. The middle layer and tapetum subsequently generated by the primary parietal layer will line the toroidal sporangium, while the protoderm (and later epidermis) defines the boundary of the anther by enveloping the columella and sporangium.

The pattern of anther wall development we observed in *Arceuthobium* is not well captured by any of Davis's (1966) four categories of anther wall ontogeny. Since no secondary parietal layer developed, the type is not basic, dicotyledonous, or monocotyledonous. And since no endothecium developed, but a middle layer did, the "reduced" category is also not appropriate. Thus, we strongly suggest that a new category, the "Arceuthobium type", be created in which *Arceuthobium* spp. might be placed.

We believe that we have clarified the processes by which the sporogenous tissue and columella develop and have explained how the mature sporangium is organized. Our observations of sporogenous tissue ontogeny do have commonalities with other descriptions (Cohen 1968; Sereda 2003). We agree that asynchronous periclinal divisions of hypodermal initials produce primary sporogenous cells toward the inside, although we further noted that archesporial cells located more deeply within the anther contribute directly to sporogenous tissue. Additionally, we have also shown that the sterile columella initiate from the deepest hypodermal layers very early in development, possibly to provide a supportive stanchion as the pollen grains separate from each other later in development. This early development of the colu-

mella generates a toroidal unilocular sporangium (and, as noted, complicates anther wall development). Similarly, Thoday and Johnson (1930) and Cohen (1968) thought the sporangium was unilocular and toroidal upon its inception, although they did not describe its relationship with columella development. Unlike Johnson (1888), Heinricher (1915), Eichler (1875), and Staedlter (1923), we do not believe that any anther septae break down or that a horseshoe-shaped sporangium becomes a ring-shaped one (Bhandari and Vohra 1983). We also do not think that the sporangium is highly variable (Pisek 1924; Dowding 1931) nor do we think that its final organization is either horseshoe shaped (Bhandari and Nanda 1968) or cup shaped (Sereda 2003). We believe that these other interpretations result from the use of oblique sections, as the anthers do not sit parallel to the long axis of the inflorescence and are also somewhat torqued. Cohen (1968) shared this view.

Microsporocytes and microsporogenesis

When the sporogenous tissue of *A. americanum* ceased dividing, the resultant microsporocytes became encased in callose-rich walls. This process of callose deposition occurs in many flowering plants and is thought to be a mechanism by which the microsporocytes become isolated from the rest of the anther tissue (Raghavan 1997). The callose, which is likely secreted by the microsporocyte protoplast, occupies the region between the plasma membrane and the original cellulosic cell wall (Rowley and Southworth 1967). Sereda (2003) did observe callose-embedded microsporocytes in *A. americanum*, but it was unclear where the callose had accumulated, because her results were confounded by plasmolysis of the microsporocytes. Our results clearly showed Aniline-Blue-positive cell wall material (likely callose) between the plasma membrane and original microsporocyte cell wall. We also noted cytomictic channels interconnecting the microsporocytes, some of them large enough (0.6 μm) to allow the passage of organelles like mitochondria. Such channels might facilitate the synchronization of cellular events in the angiosperm anther, including microsporogenesis (Heslop-Harrison 1968; Kathal et al. 1988). In *A. americanum*, the presence of callose did not occlude the cytomictic channels, which remained open even at the onset of microsporogenesis. Sumner and Remphey (2005) made a similar observation for *Amelanchier alnifolia* Nutt.

As documented by Cohen (1968), the meiotic event in *A. americanum* was rapid. In our study, microsporogenesis only took a few days to complete following the onset of prophase I and occurred at the end of August, although others reported that it took place in the fall (Cohen 1968; Hawksworth and Wiens 1996; Wiens 1968) or late July (Dowding 1931). Whether this discrepancy in timing was due to differences in host, geographical area, genetics, or seasonal variation (among other potential factors) remains to be determined. Our results otherwise support those of Sereda (2003), who noted the formation of tetrahedral tetrads by simultaneous cytokinesis. Also like Sereda (2003), we observed callose surrounding each microspore in the tetrad, likely generated by the microspores themselves (Rowley and Southworth 1967).

Prior to the separation of the microspores from the *A. americanum* tetrad, the callose wall began to dissolve. As the callose disappeared, endoplasmic reticulum in the tapetal cells became more abundant, a feature indicating that those cells had become secretory, probably releasing a callase cocktail to digest the callose. The secretion of such a cocktail has been proposed for many angiosperms and is likely tightly genetically controlled (Fei and Sawhney 1999; Frankel et al. 1969; Stieglitz and Stern 1973). While the *A. americanum* tapetal cells were interlinked through cytomictic channels, essentially forming a coenocyte, the tapetum was not sympastically connected to the microsporocytes, and so all transportation from the tapetum to the microspores would be made through the apoplasm of the loculus. Apoplastic transport

from an interlinked tapetum to the microspores is common for angiosperms (Fei and Sawhney 1999).

Microspores and microgametogenesis

Once separated from the tetrads, the uninucleate *A. americanum* microspores continued to develop. First, they increased in size. Enlargement of microspores is not uncommon for flowering plants (Piven et al. 2001; Raghavan 1997). Second, a thin autofluorescent cell wall, likely the beginning of a sporopollenin-rich exine, became apparent at the outer boundary of the recently released *A. americanum* microspores. In angiosperms, the tapetum is believed to be the source of sporopollenin, a complex mixture of lipophilic decay-resistant cell wall materials (Kathal et al. 1988). Concurrent with the first signs of sporopollenin accumulation, the tapetal cells of *A. americanum*, which had become progressively more darkly stained, became disorganized as well as warped in appearance and began to release orbicules (likely containing sporopollenin). The disorganization of the darkly staining tapetum could represent programmed cell death, another common feature of the angiosperm tapetum.

Mitosis of *A. americanum* microspores was symmetrical and more or less synchronous, generating two round nuclei of similar size and position. These nuclei were indistinguishable from each other, although one would ultimately form the vegetative nucleus, and the other, the generative nucleus. The two nuclei became rapidly partitioned from each other by the formation of a centrally located cell wall. This observation contrasts with descriptions of microgametogenesis in other flowering plants (Brown and Lemmon 1991; Kathal et al. 1988; Russell et al. 1996), in which the initial mitotic division is asymmetrical not symmetrical, and generative nuclei are often lens shaped from the outset (rather than round, as in our study). Future studies focusing on gamete formation and the fertilization process may yield interesting results, especially as the generative cell is so large relative to other angiosperms. Despite these differences, the generative cell in *A. americanum* did develop more or less like that of a typical angiosperm: as a whole, it became lens shaped with horn-like protrusions, as do the generative cells of most angiosperms, with the nucleus in *A. americanum* ultimately becoming compressed and lenticular along with the cell itself. And while vegetative nuclei of angiosperms are not typically cup shaped like those of *A. americanum*, the cytoplasmic connections expected to develop between the vegetative nucleus and generative cell (Russell and Cass 1981) might be enhanced in a cup-shaped vegetative nucleus.

Anthesis, mature pollen, and pollen dispersal

Like other authors, we found that floral initiation in *A. americanum* occurred during the previous growing season, while anthesis did not take place until the following spring; this process has been called indirect flowering (Cohen 1968; Dowding 1931; Hawksworth and Wiens 1996; Wiens 1968). As noted by Dowding (1931) and Sereda (2003), we observed that anthesis and the release of *A. americanum* pollen occurred over a three to four week period. All evidence in our study suggests that the mature pollen grains are released at the two-celled stage, a condition characteristic of the vast majority of angiosperms (Shukla et al. 1998). The micromorphology of the heterocolpate, echinate whole grains is consistent with descriptions of other species of *Arceuthobium* (Hawksworth and Wiens 1972), although our study represents the first time unprepared *Arceuthobium* grains in their native state were examined with SEM. Three true colpi or apertures alternated with three shorter pseudocolpi in which the thicknesses of the exine and intine were similar to that of the rest of the grain, and the spines were often easily 1/8 the height of the minor axis of the spheroid grains. Thus, the spikes were a predominant feature of the grains. The spheroidal nature of the grains was also particularly evident in the SEM images, with the long axis of the grain being longer than the short one by 1.25 times on average. Notably, the pollen

was also connected to each other and to the columella with a sticky pollen coat or pollenkitt. While we did not ascertain the precise chemical nature of the pollenkitt, its orange colour suggested that it was rich in carotenoids, which are characteristically present in angiosperm pollenkitt (Kathal et al. 1988). As well, during the final stages of pollen maturation, the tapetum seemed to be involved in the secretion of the pollenkitt, which is not unusual.

The presence of pollenkitt and spines on pollen is indicative of insect pollination (entomophily). Controversy has surrounded the pollination biology of *Arceuthobium* because the genus exhibits floral characteristics typical of both insect-pollinated and wind-pollinated (anemophilous) flowers (Hawksworth and Wiens 1996). We do not wish to suggest that one type of pollination predominates, as *Arceuthobium* likely simply employs both types of pollination in a generalist approach. In fact, *A. americanum* is one of the earliest-flowering species in its community, often undergoing anthesis when the temperatures are only just above freezing. Insects would not be active at these low temperatures, and so wind might be needed initially for pollination. Later, as spring progresses and the ambient temperature increases, insects might become more important. Use of both modes of pollination might also accommodate year-to-year temperature-driven fluctuations in insect activity. Yeung et al. (2011) recognized two sets of pollen in *Carthamus tinctorius* L. (safflower): pollen located next to the anther wall was “sticky”, while the centrally located pollen was more “free”. This phenomenon can account for both self-pollination and insect pollination characteristic of safflower. Whether or not this dichotomy occurs in *Arceuthobium* warrants further examination.

As mentioned, unusual to the development of the *A. americanum* anther wall is the development of fibrous thickenings in the epidermal layer along with the absence of an endothecium. The exothecium in *A. americanum* seems to play the same general role as a typical endothecium, allowing the anther to open and release pollen via the dehydration of a fibrous layer, which subsequently permits the anther wall to roll back upon itself along a line of weakness (Skene 1948). In *A. americanum*, we observed that this line of weakness corresponded to the area where the long axis of the columella’s head contacted the top of the anther. Thus, in addition to possibly functioning as a stanchion, the columella might play a key role in anther dehiscence. *Arceuthobium americanum* is unusual in its possessing the ability to close its anthers in response to low temperature and increased humidity, which might help to protect and conserve pollen (Gilbert and Punter 1990). We noted that initial pollen release was explosive upon anther opening but that some pollen remained behind, glued to the columella by pollenkitt. This reservation of pollen suggests again that initial dispersal is by wind, followed later by insect-guided dissemination. The anther of *Ricinus communis* L., which also possesses an exothecium, employs a similar method of pollen dispersal: the initial dispersive event is explosive, but some pollen remains behind glued to a central septum via pollenkitt (Bianchini and Pacini 1996). The central septum seems to play the same role positioned for the *A. americanum* columella, although the *R. communis* anthers do not reclose. Pollen dispersal in angiosperms is not usually explosive, and *R. communis* is the only species in which explosive pollen dispersal is attributable to anthers; in the few other angiosperms with explosive pollen dispersal (e.g., *Parietaria officinalis* L.), the discharge is due to motion of the filament rather than the anther (Skene 1948).

Other angiosperms that lack an endothecium and instead have an exothecium can be found in the family Ericaceae, specifically *Kalmia* L. and *Phyllodoce* Salisb. (Davis 1966; Kron et al. 2002; Skene 1948). However, in these Ericaceae, the pollen dispersal mechanism is quite different (formation of a pore rather than a slit) from that of *A. americanum*. The absence of an endothecium and development of an exothecium is characteristic of gymnosperms, excepting *Ginkgo* L. (Bhatnagar and Moitra 1996). The absence of an

endothecium in the gymnosperms is believed to be the primitive condition and not a derived state arising from the loss of the endothecium as it is in the angiosperms (Skene 1948). The mechanism for gymnosperm pollen dispersal, however, is similar to that of most angiosperms and not particularly explosive. In contrast, leptosporangiate ferns seem to show the opposite extreme, having extremely explosive pollen dispersal. However, these ferns employ a catapult-like motion in which the majority of dispersal is accomplished on the second “return” motion, not the first “pull-back” one. When compared with all of these types of plants, therefore, it is safe to conclude that the type of explosive pollen dispersal seen in *A. americanum* is highly unusual.

Conclusion

Our study has gone a long way toward elucidating anther and pollen development in *A. americanum*. We clearly described anther and pollen anatomy throughout development and resolved the inconsistencies of earlier reports, such as the conflicting descriptions for the origin and shape of the microsporangium and columella. We demonstrated that the microsporangium is toroidal from the outset and that anther wall development involves the columella. We explained how the columella arises and likely functions in structural support as well as pollen dispersal. To our knowledge, the type of anther wall development we described for *A. americanum* has not been seen in other angiosperms, and hence, we suggest that a new category of wall development, the *Arceuthobium* type, be used. We also revealed key aspects of microsporogenesis and microgametogenesis, such as how and when callose appears as well as how the generative and vegetative cells, which are not typical for angiosperms, manifest. Anther wall development as well as male gametophyte organization is so different from other angiosperms that these anomalies warrant deeper examination in future studies, perhaps with a focus on genetics and an eye on dwarf mistletoe control. Similar to most other angiosperms, the *A. americanum* tapetum is the secretory type, and pollen grains are shed at the two-celled stage. In our study, the heterocolpate, echinate pollen grains of *A. americanum* were seen for the first time with SEM in their native, unprepared state. This work contributes to the understanding of *A. americanum*, the genus *Arceuthobium*, and angiosperms as a whole.

Acknowledgements

The research was funded by a Natural Sciences and Engineering Research Council of Canada Discovery Grant provided to CMRF. We heartily thank Nancy Flood (Department of Biological Sciences) at Thompson Rivers University for editing the earliest draft of the manuscript. We also graciously acknowledge Karen Yvonne Sereda, who collected and processed Manitoba samples that were used to augment the results of this work. Thanks also to Kayla Holtslag, who helped prepare and check the references.

References

- Anjaneyulu, C., and Lakshminarayana, K. 1989. Microsporogenesis and the development of male gametophyte in two species of *Diospyros* L. *Taiwania*, 34(2): 187–191. doi:10.2307/2440467.
- Bhandari, N.N. 1984. The microsporangium. In *Embryology of angiosperms* [online]. Edited by B. Johri. Springer Berlin Heidelberg, Germany. pp. 53–121. doi:10.1007/978-3-642-69302-1_2.
- Bhandari, N.N., and Nanda, K. 1968. Studies in the Viscaceae. II. A reinvestigation of the female gametophyte of *Arceuthobium douglasii*. *Am. J. Bot.* 55(9): 1028–1030. doi:10.2307/2440467.
- Bhandari, N., and Vohra, C. 1983. Embryology and affinities of Viscaceae. In *The biology of mistletoes*. Edited by D.M. Calder and P. Bernhardt. Academic Press, New York, USA. pp. 69–86.
- Bhatnagar, S., and Moitra, A. 1996. *Gymnosperms*. New Age International, New Delhi, India.
- Bianchini, M., and Pacini, E. 1996. The caruncle of *Ricinus communis* L. (castor bean): its development and role in seed dehydration, rehydration, and germination. *Int. J. Plant Sci.* 157(1): 40–48. doi:10.1086/297318.
- Brown, R.C., and Lemmon, B.E. 1991. Pollen development in orchids. 1. Cytoskel-

- eton and the control of division plane in irregular patterns of cytokinesis. *Protoplasma*, **163**(1): 9–18. doi:10.1007/BF01323402.
- Chhikara, A., and Ross Friedman, C.M. 2008. The effects of male and female *Arceuthobium americanum* (lodgepole pine dwarf mistletoe) infection on the relative positioning of vascular bundles, starch distribution, and starch content in *Pinus contorta* var. *latifolia* (lodgepole pine) needles. *Botany*, **86**(5): 539–543. doi:10.1139/B08-019.
- Cohen, L.I. 1968. Development of the staminate flower in the dwarf mistletoe, *Arceuthobium*. *Am. J. Bot.* **55**(2): 187–193. doi:10.2307/2440451.
- Davis, G.L. 1966. Systematic embryology of the angiosperms. John Wiley & Sons, New York, USA.
- Dowding, E.S. 1931. Floral morphology of *Arceuthobium americanum*. *Bot. Gaz.* **91**(1): 42–54. doi:10.1086/334124.
- Eichler, A.W. 1875. Blüthendiagramme. W. Engelmann, Leipzig, Germany. doi:10.5962/bhl.title.12323..
- Fei, H., and Sawhney, V.K. 1999. MS32-regulated timing of callose degradation during microsporogenesis in *Arabidopsis* is associated with the accumulation of stacked rough ER in tapetal cells. *Sex. Plant Reprod.* **12**(3): 188–193. doi:10.1007/s004970050191.
- Frankel, R., Izhar, S., and Nitsan, J. 1969. Timing of callase activity and cytoplasmic male sterility in *Petunia*. *Biochem. Genet.* **3**(5): 451–455. doi:10.1007/BF00485605. PMID:5358139.
- Gilbert, J., and Punter, D. 1990. Release and dispersal of pollen from dwarf mistletoe on jack pine in Manitoba in relation to microclimate. *Can. J. For. Res.* **20**(3): 267–273. doi:10.1139/x90-039.
- Godfree, R.C., Tinnin, R.O., and Forbes, R.B. 2002. The effects of dwarf mistletoe, witches' brooms, stand structure, and site characteristics on the crown architecture of lodgepole pine in Oregon. *Can. J. For. Res.* **32**(8): 1360–1371. doi:10.1139/x02-058.
- Gonzalez, F., Rudall, P.J., and Furness, C.A. 2001. Microsporogenesis and systematics of Aristolochiaceae. *Bot. J. Linn. Soc.* **137**(3): 221–242. doi:10.1111/j.1095-8339.2001.tb01119.x.
- Hawksworth, F.G., and Wiens, D. 1972. Biology and classification of dwarf mistletoe (*Arceuthobium*). U.S. Department of Agriculture, Agriculture Handbook 401. U.S. Department of Agriculture, Washington, D.C., USA.
- Hawksworth, F.G., and Wiens, D. 1996. Dwarf mistletoes: biology, pathology, and systematics. Diane Publishing, Darby, Pa., USA.
- Heide-Jørgensen, H.S. 2008. Parasitic flowering plants. Brill, Leiden, Netherlands.
- Heinricher, E. 1915. Contributions to the biology of dwarf mistletoe, *Arceuthobium oxycedri*, especially the knowledge of the anatomical structure and the mechanics of their explosive berries. *Sber His Imp. Wiss.* **124**: 181–230. Available from <http://kdb.kew.org/kdb/detailedresult.do?id=8893> [accessed 25 September 2013].
- Heslop-Harrison, J. 1968. Pollen wall development. *Science*, **161**(3838): 230–237. doi:10.1126/science.161.3838.230. PMID:5657325.
- Johnson, T. 1888. *Arceuthobium oxycedri*. *Ann. Bot.* **os-2**(2): 137–160. doi:10.1093/aob/os-2.2.137.
- Kathal, R., Bhatnagar, S.P., and Bhojwani, S.S. 1988. Regeneration of plants from leaf explants of *Cucumis melo* cv. *Pusa Sharbati*. *Plant Cell Rep.* **7**(6): 449–451. PMID:24240267.
- Kron, K.A., Judd, W.S., Stevens, P.F., Crayn, D.M., Anderberg, A.A., Gadek, P.A., Quinn, C.J., and Luteyn, J.L. 2002. Phylogenetic classification of Ericaceae: molecular and morphological evidence. *Bot. Rev.* **68**(3): 335–423. doi:10.1663/0006-8101(2002)068[0335:PCOEMA]2.0.CO;2.
- O'Brien, T.P., and McCully, M.E. 1981. The study of plant structure: principles and selected methods. Termarcarphi Pty. Ltd., Melbourne, Australia.
- Penfield, F.B., Stevens, R.E., and Hawksworth, F.G. 1976. Pollination ecology of three Rocky Mountain dwarf mistletoes. *For. Sci.* **22**: 473–484.
- Pisek, A. 1924. Antherenentwicklung und meiotische Teilung bei der Wacholdermistel [*Arceuthobium oxycedri* (DC) M.B.]: Antherenbau und Chromosomenzahlen von *Loranthus europaeus* Jacq. *Akad. Wiss. Wien Sitzungsber., Math.-Naturwiss. Kl., Abt. 1.* **133**: 1–15.
- Piven, N.M., Barredo-Pool, F.A., Borges-Argáez, I.C., Herrera-Alamillo, M.A., Mayo-Mosqueda, A., Herrera-Herrera, J.L., and Robert, M.L. 2001. Reproductive biology of henequen (*Agave fourcroydes*) and its wild ancestor *Agave angustifolia* (Agavaceae). I. Gametophyte development. *Am. J. Bot.* **88**(11): 1966–1976. doi:10.2307/3558424. PMID:21669630.
- Polhill, R.M., and Wiens, D. 1999. Flora of tropical East Africa: prepared at the Royal Botanic Gardens, Kew with assistance from the East African Herbarium. Visceaeae. Edited by H. Beentje and C.M. Whitehouse. Balkema, Rotterdam, Netherlands.
- Raghavan, V. 1997. Molecular embryology of flowering plants. Cambridge University Press, Cambridge, UK.
- Ross, C.M., and Sumner, M.J. 2004. Development of the unfertilized embryo sac and pollen tubes in the dwarf mistletoe *Arceuthobium americanum* (Visceaeae). *Can. J. Bot.* **82**(11): 1566–1575. doi:10.1139/b04-121.
- Rowley, J., and Southworth, D. 1967. Deposition of sporopollenin on lamellae of unit membrane dimensions. *Nature*, **213**: 703–704. doi:10.1038/213703a0.
- Russell, S.D., and Cass, D.D. 1981. Ultrastructure of the sperms of *Plumbago zeylanica*. *Protoplasma*, **107**(1–2): 85–107. doi:10.1007/BF01275610.
- Russell, S.D., Strout, G.W., Stramski, A.K., Mislan, T.W., Thompson, R.A., and Schoemann, L.M. 1996. Microgametogenesis in *Plumbago zeylanica* (Plumbaginaceae). 1. Descriptive cytology and three-dimensional organization. *Am. J. Bot.* **83**(11): 1435–1453. doi:10.2307/2446099.
- Sereda, K.Y. 2003. Phenology of anther development of dwarf mistletoe (*Arceuthobium americanum* Nutt. ex Engelm.): an anatomical investigation of microsporogenesis and microgametogenesis. M.Sc. thesis, University of Manitoba, Winnipeg, Man., Canada.
- Shukla, A., Vijayaraghavan, M., and Chaudhry, B. 1998. Biology of pollen. APH Publishing, New Delhi, India.
- Skene, M. 1948. Biology of flowering plants. Discovery Publishing House, New Delhi, India.
- Spurr, A.R. 1969. A low-viscosity epoxy resin embedding medium for electron microscopy. *J. Ultrastruct. Res.* **26**: 31–43. doi:10.1016/S0022-5320(69)90033-1. PMID:4887011.
- Staedler, G. 1923. Über Reduktionserscheinungen im Bau der Antherenwand von Angiospermen-Blüten. *Flora (Jena)*, **16**: 85–108.
- Stewart, C.D., and Ross, C.M. 2006. Embryological and phenological comparison between *Arceuthobium americanum* (the lodgepole pine dwarf mistletoe) growing on *Pinus contorta* var. *latifolia* in British Columbia and on *P. banksiana* in Manitoba. *Davidsonia*, **17**(4): 107–115.
- Stieglitz, H., and Stern, H. 1973. Regulation of β -1,3-glucanase activity in developing anthers of *Lilium*. *Dev. Biol.* **34**(1): 169–173. doi:10.1016/0012-1606(73)90347-3. PMID:4787601.
- Sumner, M.J., and Remphrey, W.R. 2005. Microsporogenesis in *Amelanchier alnifolia*: sporogenous cells, microsporocytes, and tetrads. *Can. J. Bot.* **83**(9): 1106–1116. doi:10.1139/b05-079.
- Sutherland, J., and McCully, M.E. 1976. A note on the structural changes in the walls of pericycle cells initiating lateral root meristems in *Zea mays*. *Can. J. Bot.* **54**(17): 2083–2087. doi:10.1139/b76-222.
- Thoday, D., and Johnson, E.T. 1930. On *Arceuthobium pusillum*, Peck: I. The endophytic system. *Ann. Bot.* **44**(2): 393–413. Available from <http://aob.oxfordjournals.org/content/os-44/2/393.short> [accessed 25 September 2013].
- Wiens, D. 1968. Chromosomal and flowering characteristics in dwarf mistletoes (*Arceuthobium*). *Am. J. Bot.* **55**(3): 325–334. doi:10.2307/2440419.
- Willemse, M.T.M. 1972. Changes in the autofluorescence of the pollen wall during microsporogenesis and chemical treatments. *Acta Bot. Neerl.* **21**: 1–16.
- Wilson, C.A., and Calvin, C.L. 1996. Anatomy of the dwarf mistletoe shoot system. In *Dwarf mistletoes: biology, pathology, and systematics*. Chap. 10. Edited by F.G. Hawksworth and D. Wiens. pp. 95–111. Available from http://www.fs.fed.us/rm/pubs_other/rmrs_1996_hawksworth_f001/rmrs_1996_hawksworth_f001_10.pdf [accessed 25 September 2013].
- Yeung, E.C., Oinam, G.S., Yeung, S.S., and Harry, I. 2011. Anther, pollen and tapetum development in safflower, *Carthamus tinctorius* L. *Sex. Plant Reprod.* **24**(4): 307–317. doi:10.1007/s00497-011-0168-x. PMID:21573927.